FISEVIER

Contents lists available at ScienceDirect

International Journal of Heat and Mass Transfer

journal homepage: www.elsevier.com/locate/ijhmt





True benefits of multiple nanoparticle sizes in radiative cooling paints identified with machine learning

Daniel Carne ^a, Joseph Peoples ^a, Fredrik Arentz ^a, Xiulin Ruan ^{a,*}

^a School of Mechanical Engineering, Purdue University, West Lafayette, IN 47907, USA

ARTICLE INFO

Keywords: Radiative cooling Machine learning Optimization

ABSTRACT

Previous works find that multiple nanoparticle sizes in radiative cooling paints increase solar reflectance compared to a single particle size. In this study, we assess this finding by combining Mie theory, Monte Carlo simulations, and machine learning methods to identify the optimum particle size combinations in BaSO $_4$ and TiO $_2$ -acrylic radiative cooling paints. We have found that the optimal multiple particle sizes indeed outperform the optimal single size in TiO $_2$ paint, but surprisingly underperform compared to the optimal single size in BaSO $_4$ paint. This is due to the near constant refractive index of BaSO $_4$ across the solar spectrum. Also, different particle size distributions yield similarly high solar reflectance as long as the average particle size is in the neighborhood of 300–600 nm. Considering that it is unfeasible to precisely manufacture a single particle size, we conclude that the true benefits of multiple particle sizes is that they enable cost effective manufacturing while preserving robust high performance.

1. Introduction

Space cooling currently accounts for 11 % of the total energy use in residential buildings in the US and is expected to increase to 16 % in 2050 [1]. This increase, along with the increase in the number of buildings, will put additional demand on the electricity grid as well as exacerbate the urban heat island effect. To meet these demands as well as to provide efficient cooling methods where electricity is not as available, passive cooling technologies can be used which do not require energy input. Radiative cooling paint can provide passive cooling by a combination of reflecting greater than 85 % of solar heating and emitting radiation into the deep space through the atmospheric sky window. For every 1 % increase in solar reflectance, passive cooling increases by about 10 W/m^2 , allowing for up to 150 W/m^2 of cooling with an ideal emitter [2]. With recent advancements in materials and electromagnetic interactions at the nano scale, radiative cooling paints have made significant strides towards providing viable passive cooling.

Early pursuits of radiative cooling paints were limited by their performance [3–6]. More recent works have engineered a variety of factors, including the pigment material, particle size, size distribution, and concentration to achieve enhanced radiative properties in a single layer [2,7–9]. Wang et al. showed TiO_2 particle agglomeration reduces solar reflectance and should be minimized [10]. Peoples et al. predicted large

differences in solar reflectance using varying size nanoparticles in TiO2 paint due to different particle sizes reflecting different portions of the solar spectrum more efficiently [2]. This work concluded that a combination of particle sizes can increase a paint's reflectance due to the broadband nature of the solar spectrum. Multiple other works including Chen et al. [11], Dong et al. [12], and Wang et al. [13] have reached the same conclusion that a combination of particle or pore sizes increase solar reflectance over a single particle size. The concept was used by Li et al. in achieving a remarkable 98.1 % solar reflectance with a single layer BaSO₄ paint due to BaSO₄ having no absorption within the solar spectrum, where a distribution of particle size was shown to yield higher solar reflectance than a single particle size again [8]. It should be noted that some of these works compared a distribution to a single size at the average size of the size distribution as obtained in experiments, while it was unclear whether that is the optimal single size. Especially for novel radiative cooling paint materials such as BaSO4, little is known on what the optimal single particle size and multiple particle size combinations are. Therefore, it warrants study to optimize single size and multiple sizes, and evaluate whether multiple sizes always enhance solar reflectance.

In this study, we examine the role nanoparticle size plays on $BaSO_4$ and TiO_2 radiative cooling paint. Initially, the spectral response of varying nanoparticle sizes is examined to build an understanding about

E-mail address: ruan@purdue.edu (X. Ruan).

^{*} Corresponding author.

the system. The optimum single nanoparticle size at different paint thicknesses is determined so that the optimal single size is known for comparison purposes. Then, starting near the optimal single nanoparticle size, an additional nanoparticle size is added and optimized through an evolutionary algorithm as well as a brute force search to determine the optimal combination of nanoparticle sizes. Due to manufacturing constraints to make an affordable paint, nanoparticle sizes will be within a certain distribution. The effect of this distribution across different size particles is examined, and the benefits of such distribution are discussed and updated from previous understanding in terms of meeting manufacturing constrains while preserving similarly high solar reflectance.

2. Methodology

Determining the spectral response of a nanoparticle medium can be a computationally expensive task, hindering efforts to quickly ascertain optimal particle size combinations. In this study, Mie theory is used to calculate the optical properties of each individual particle size from the material properties. The material properties required are the refractive index and the extinction coefficient. Both the TiO₂ and BaSO₄ properties used are the same as from previous works on these paints and should be noted that the BaSO₄ refractive index is estimated with a Drude model [2,8]. In this work, we propose two separate methods to efficiently determine the ideal nanoparticle size combination. The first method applies Monte Carlo simulations and a pre-trained deep neural network with the optical properties to model photon transport. However, due to computational limitations, an optimization algorithm is required to find the optimal combination of particle sizes. The second method, a reduced order analysis with several assumptions is computationally efficient enough to perform a bulk force search of all particle size combinations at set intervals. This second method will help to confirm the optimization method is not stuck in a local maximum.

2.1. Mie theory and effective medium theory

Mie theory is an analytical solution to Maxwell's equations for electromagnetic wave interaction in homogenous spherical particles where the diameter is comparable to the photon wavelength. In this work, we use Mie theory formulated for an absorbing medium by Frisvad et al. [14]. By providing the complex index of refraction of the nanoparticle and matrix, the scattering coefficient, absorption coefficient, and asymmetry parameter can be calculated for a single particle. Then, effective medium theory can be used to create an effectively homogenous medium with volume averaged properties [2,6] along with a dependent scattering correction at volume fractions greater than 8 % [15]. The dependent scattering correction by Kamiuto [16] for packed sphere beds is applied where both the absorption and scattering coefficient are adjusted by:

$$\mu_{corrected} = \mu \left(1 + \frac{3}{2}f - \frac{3}{4}f^2 \right) \tag{1}$$

where μ is the independent scattering or absorption coefficient, and f is the volume fraction of nanoparticles. In this work, the absorption coefficient includes the absorption from the matrix the nanoparticles are embedded in by:

$$\mu_a = \mu_{a,p} + \frac{4\pi k_m}{\lambda (1 - f)} \tag{2}$$

where μ_{ap} is the absorption coefficient of the medium due to the embedded nanoparticles, k_m is the extinction coefficient of the matrix, and λ is the photon wavelength [14,17].

2.2. Monte Carlo photon transport

Monte Carlo simulations can model the radiative transport equation for scattering and absorbing media by tracking photon packets, and stochastically modeling the probabilistic events such as scattering angle and step size [18]. This method is commonly applied to radiative heat transfer problems, as well as specifically for radiative cooling paints [7, 8,18,19]. While far more efficient than directly solving Maxwell's equations, Monte Carlo simulations are still computationally intensive. In this work, a Monte Carlo program based off the process described in Wang et al. is used to calculate the spectral response, including the reflectance, absorptance, and transmittance [20]. The solar reflectance is then calculated by integrating the spectral reflectance with the AM1.5 solar spectrum [21].

2.3. Reduced order analysis

Due to the complexity of Monte Carlo simulations, which requires the effective medium's refractive index, scattering coefficient, absorption coefficient, asymmetry parameter, and thickness as inputs, there is not a simple method to curve fit this data for fast analysis and optimization. To reduce the number of dimensions for radiative cooling paint optimization, several assumptions can be made. First, to remove the absorption coefficient, it is assumed the matrix is non-absorbing. For the acrylic based paint, the absorption within the solar spectrum due to the matrix is generally less than 2 %. Second, to remove the refractive index as a variable, it is assumed the matrix the nanoparticles are embedded in has a constant index of refraction of 1.5. For acrylic based paint this value ranges between 1.48 and 1.56. Third, to combine the scattering coefficient and asymmetry parameter, a reduced scattering coefficient is defined as:

$$\mu_s' = \mu_s(1 - g) \tag{3}$$

where μ_s is the scattering coefficient and g is the asymmetry parameter. This approach has been used before [22,23], and testing with radiative cooling paint examples show negligible difference with this method. With these three assumptions, the reflectance of a medium at a specific wavelength is now only a function of the reduced scattering coefficient. Using effective medium theory [24], the reduced scattering coefficient for a medium with multiple different size nanoparticles can be calculated by:

$$\mu'_{s} = \sum_{i=1}^{n} \frac{3f_{i}Q_{sca,i}(1-g_{i})}{2d_{i}} \tag{4}$$

where i is an index for each particle size, n is the number of different particle sizes used, $Q_{sca,i}$ and g_i are the scattering efficiency and asymmetry parameter of an individual particle calculated using Mie theory, and f_i and d_i are the volume fraction and diameter corresponding to that particle size respectively. Using a small number of Monte Carlo simulations at a constant thickness, a spline fit can be used to estimate the reflectance at each wavelength based only on the reduced scattering coefficient calculated by Eq. (4), significantly reducing the computational power required.

2.4. Evolutionary algorithm

Evolutionary algorithms are regularly used in optimization problems with multiple maxima/minima by replicating nature's process of "survival of the fittest" [25]. This process works by creating a population of individuals with traits, where each trait is a variable in the system. Each individual is evaluated with a fitness function that selects the top individuals to then create a new generation. The traits of these top individuals are mutated as they are passed down to the next generation, creating a new set of individuals with unique traits. In this study, an

evolutionary algorithm with momentum [26] will be used to optimize the particle sizes and volume fractions by:

$$x_i^{t+1} = x_i^t \left(1 + 2\alpha \left(rand - \frac{1}{2} \right) \right) + \beta \left(x_i^t - x_i^{t-1} \right)$$
 (5)

where x represents an individual which is a set of traits, the subscript i refers to one of the individual's traits such as nanoparticle size or volume fraction, the superscript t is the generation, α is the ratio of x_t a trait can mutate within, β is the momentum term, and *rand* is a random number between zero and one. Ideally the evolutionary algorithm would evaluate each individual's fitness as the solar reflectance calculated through Mie theory in combination with Monte Carlo simulations, however highfidelity Monte Carlo simulations are too computationally expensive for an iterative optimization method. Instead, for the first 250 generations, a deep neural network which has been pre-trained on radiative cooling paints is used to replace the Monte Carlo simulations [27]. This will allow for fast optimization to approximate the ideal particle sizes and volume fractions and provide good initial conditions. Then, the next 50 generations will use Monte Carlo simulations with 300,000 photons (with a standard deviation in solar reflectance of 0.02 %) to discover the true optimal the sizes and volume fractions. The combination of machine learning and Monte Carlo simulations will allow for accelerated optimization while still providing high quality results.

3. Results and discussion

To better understand directly how nanoparticle size affects spectral reflectance, several paint examples are shown in Fig. 1. Fig. 1(A) shows four different BaSO₄-acrylic and TiO₂-acrylic paints varying the diameter of the nanoparticles from 200 to 1600 nm. For both paints, the smaller nanoparticles have the highest reflectance at shorter wavelengths while the larger nanoparticles have the highest reflectance at longer wavelengths. Fig. 1(B) shows the spectral reflectance for four different thickness of BaSO4-acrylic paints with the nanoparticle diameter held constant. As the thickness increases, the reflectance increases and the returns eventually diminish. This is due to the transmission, which decreases exponentially as the thickness increases and cannot be further reduced. Based on this knowledge and previous literature, we theorize that BaSO₄-acrylic paints will benefit from multiple particle sizes to achieve high reflectance for two arguments. One, due to the broadband nature of solar irradiation, multiple particle sizes can more efficiently reflect different regions of the solar spectrum. Two, as a paint's reflectance increases, a single particle size's reflectance will reach diminishing return whereas a separate particle size may provide regions in the spectrum with higher returns. Additionally, it is important

to note that this study does not consider particle agglomeration and assumes particles are dispersed within the matrix.

3.1. Single nanoparticle optimization

First, the optimal single particle size will be determined. As the particle size varies between 250 and 10,000 nm for BaSO₄-acrylic paint, only one maximum exists. Fig. 2 shows the solar reflectance as a function of nanoparticle size for five different thicknesses. The optimal single nanoparticle size range that gives a reflectance within 0.0005 of the peak reflectance for each paint thickness is shown. At a paint thickness of 50 μ m, the optimal nanoparticle size is 435 nm, but as the paint thickness increases to 800 μ m the optimal nanoparticle size is 515 nm (Fig. S1). This confirms previous intuition as when the reflectance is lower at the smaller thicknesses, it is better to choose a nanoparticle size that reflects the peak wavelength of the solar irradiation. However, as the reflectance increases and returns diminish, it is better to choose a nanoparticle size with a broader reflectance spectrum. Fig. 2 also shows that as the paint thickness increases, the range of particle sizes that will provide similar reflectance values widens due to diminishing returns.

However, any single size nanoparticle between 400 and 530 nm provided a solar reflectance within 0.002 of the maximum for each thickness tested, so optimization for different thicknesses is not crucial to a paint's performance as long as the nanoparticle size is within an acceptable range.

3.2. Multiple nanoparticle optimization

Using the evolutionary algorithm described in the methods section, ${\rm BaSO_4}$ and ${\rm TiO_2}\text{-}{\rm acrylic}$ paint are optimized with two different nanoparticle sizes with a pre-trained neural network for the first 250 generations, then with Monte Carlo simulations for the last 50 generations. Poor initial conditions are used to test the robustness of the algorithm, starting with one 25 nm particle and one 2000 nm particle. The evolutionary algorithm reduces the volume fraction of particle 2 to 0 % leaving only a single particle size for both BaSO₄ and TiO₂. The single particle remaining converges to the expected optimal single size (Fig. S2).

This problem is commonly seen in optimization as the solution found was a local optimum but not the global optimum. This process is repeated where the initial two nanoparticle sizes are set at 0.2 and 0.6 μ m, which is near the ideal solution. Here, to compare at similar solar reflectance values, the TiO₂ maximum volume fraction is limited to 10 % while the BaSO₄ maximum volume fraction is limited to 60 %. For the TiO₂ paint the solution converges to two particles sizes sharing the total

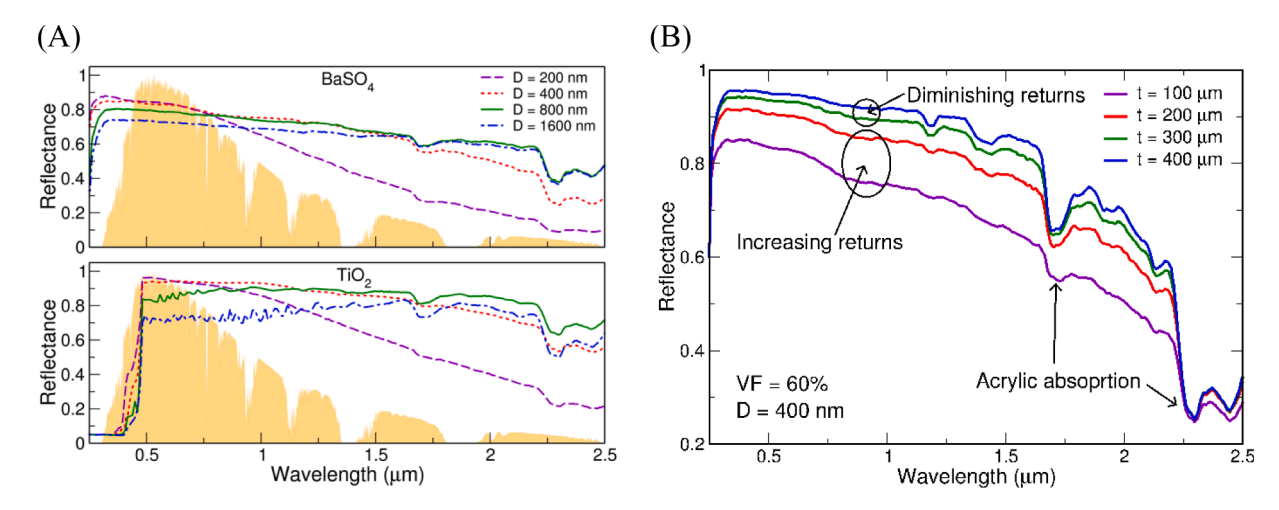


Fig. 1. (A) Spectral reflectance for a few nanoparticle sizes from 200 to 1600 nm in 100 μm thick BaSO₄-acrylic paint with a 60 % volume fraction and 25 μm thick TiO₂-acrylic paint with a 30 % volume fraction; (B) Spectral reflectance for four different thicknesses ranging from 100 to 400 μm of BaSO₄-acrylic paint.

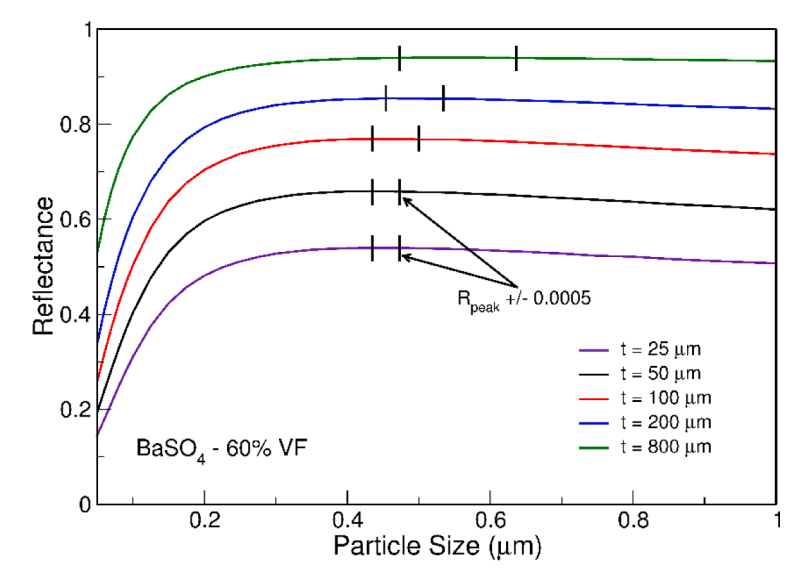


Fig. 2. Solar reflectance of BaSO $_4$ -acrylic paint as a function of particle size with a 60 % volume fraction for a few different thicknesses from 25 to 800 μ m. The bars on each curve show the range of particle sizes with a reflectance within 0.0005 of the peak reflectance.

volume fraction as seen in Fig. 3(B). Using Monte Carlo simulation with 1,000,000 photons (standard deviation in solar reflectance of 0.005 %), these results are confirmed showing the TiO₂ particle combination found has a 0.87 % higher solar reflectance over the optimal single particle size. However, for BaSO₄ paint the two-particle optimization does not find an improved solution over the single particle optimization as seen in Fig. 3(A). This is surprising as previous literature as well as the intuition developed from Fig. 1 suggests multiple particle sizes should increase the solar reflectance. To confirm these results as well as to test if multiple particle sizes are beneficial at thicker paints where the reflectance is higher, the reduced order analysis described in the methods section is applied. As this relies on spline interpolation instead of Monte Carlo simulations for each wavelength, the computational speedup allows for a brute force. A 1000 µm thick paint is examined where every combination of two nanoparticle sizes is tested with the respective volume fraction between 0 and 60 % with intervals of 2 % (total volume fraction kept at 60 %), and the nanoparticle diameter limited between 40 and 1000 nm with intervals of 40 nm. The optimal solution found provides a solar reflectance of 0.96 with a 58 % volume fraction of 520 nm particles and 2 % volume fraction of 480 nm particles. A Monte Carlo simulation using a non-absorbing acrylic medium provides a solar reflectance of 0.96 using this solution, showing the difference between these two methods are negligible for non-absorbing paints. Since this method is restricted to 40 nm intervals, this is repeated with 1 nm intervals between 480 and 520 nm. With the refined intervals, the optimal solution is a single 518 nm size nanoparticle, confirming a single size is ideal for BaSO₄ paints. Additionally, calcium carbonate pigment and air pores are examined to build a better understanding of if TiO2 is unique in that multiple particle sizes are ideal, or if BaSO₄ is unique in having a single optimal size. In Fig. 3(C) and 3(D) we see for CaCO₃ and air pores the two-particle optimization does not find a solution that improves the solar reflectance over the single particle size optimum.

With these results, we conclude that for $BaSO_4$ radiative cooling paint, multiple particle sizes do not increase the solar reflectance as compared to the optimal single size particle, contrary to previous understanding. There are multiple reasons this may be seen. First, if multiple particle sizes are tested without the optimal single particle size being known, results may indicate a higher solar reflectance than the non-optimal single particle sizes that are being used as the comparison. This result may not hold true if the optimal single particle size was determined and tested as well. The main reason, however, is due to the change in refractive index over the solar spectrum. The large change in

the refractive index of ${\rm TiO_2}$ creates a high sensitivity to changes in particle size in the reduced scattering coefficient at the shorter wavelengths but a low sensitivity at longer wavelengths as seen in Fig. 4. BaSO₄, CaCO₃, and air pores have relatively little to no change in refractive index across the solar spectrum, so the sensitivity to particle size stays similar across the spectrum. Due to the change in particle size sensitivity in the ${\rm TiO_2}$ reduced scattering coefficient, the benefits seen from different particle sizes reflecting different regions in the solar spectrum are amplified. From this trend, we theorize that when there is an appreciable change in refractive index across the solar spectrum for low absorbing dielectric nanoparticles, multiple particle sizes may be beneficial.

3.3. Nanoparticle size distribution

Due to the processes involved in manufacturing nanoparticles it is not realistic to expect a single size nanoparticle, but rather a distribution. Especially when developing a radiative cooling paint, the cost of manufacturing can limit a paint's commercial potential. While TiO2 particle size distributions have been studied previously [28], little is known as to how a distribution will affect the radiative properties for BaSO₄ paint. For this study, 101 individual particle sizes are used to model the distribution where the minimum and maximum individual particle size used is +/-45 % of the mean particle size. The volume fraction of each particle size follows a Gaussian distribution where +/-45 % of the mean particle size is two times the standard deviation. Fig. 5 shows the effect of different distributions at different mean nanoparticle sizes for a lower and higher reflectance example of BaSO4 and TiO2-acrylic paint. For both the thin and thick examples, the distribution provides similarly high solar reflectance as the single size particle. The thin and thick examples volume fraction and thickness were selected to provide a similar solar reflectance between pigments. This contrasts with Ref. [2], a previous study from our group, which showed a nanoparticle distribution increases TiO₂ solar reflectance. When simulating the same case as Ref. [2] (2000 μ m, 8 % volume fraction, 104 +/- 37 nm particles) where the acrylic absorption is not considered, similar results are seen as theirs where the distribution does increase the reflectance. However, a distribution does not increase the reflectance when the absorption in acrylic is considered. For both BaSO₄-acrylic and TiO2-acrylic paint, the broadband nature of the solar spectrum along with the diminishing returns at high reflectance values allow for the distribution to provide similarly high reflectance even though

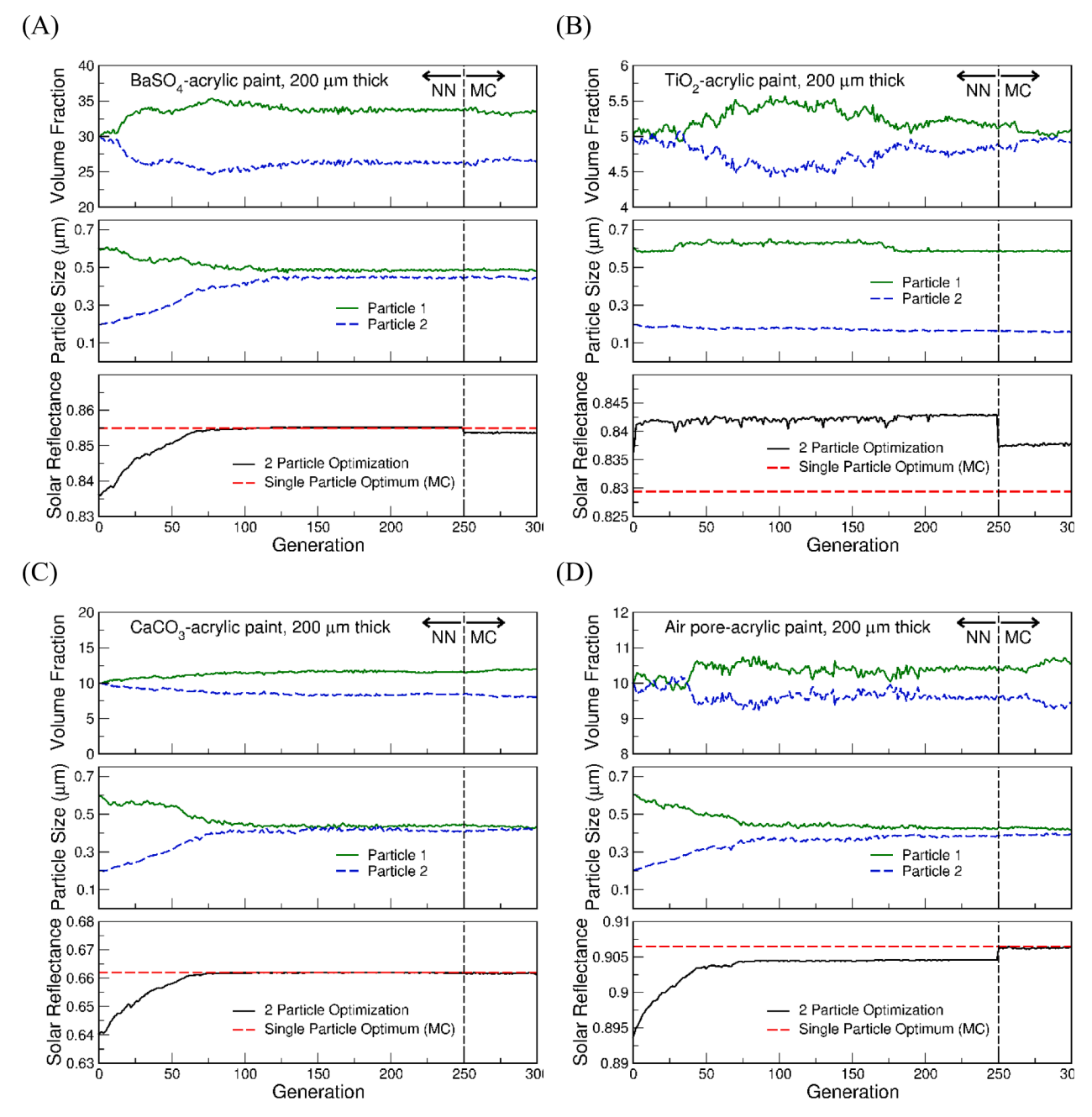


Fig. 3. Evolution of two particle sizes, their respective volume fractions, and the resulted solar reflectance for (A) BaSO₄-acrylic paint at a 60 % volume fraction, (B) TiO₂-acrylic paint at a 10 % volume fraction, (C) CaCO₃-acrylic paint at a 20 % volume fraction, and (D) Air pore-acrylic paint at a 20 % volume fraction.

non-optimal sized particles are utilized.

4. Conclusion

In this work, we investigate the role of multiple nanoparticle sizes and distributions in radiative cooling paint. Previous works, and our own intuition, indicate that multiple particle sizes increase solar reflectance compared to a single particle size due to the broadband nature of the solar spectrum. We have found that optimized multiple particle sizes do indeed increase solar reflectance over a single optimal particle size for TiO₂-acrylic paint, but not for BaSO₄-acrylic paint due to the near constant refractive index of BaSO₄ across the solar spectrum. We have also found that a particle size distribution at the optimal mean particle size has negligible effects on solar reflectance for both BaSO₄ and TiO₂-acrylic paint. Considering that it is unfeasible or too expensive

to precisely accomplish a single particle size in manufacturing processes, we conclude that contrary to previous understanding, the true benefits of particle size distributions in radiative cooling paints with low absorption dielectric nanoparticles are that they enable cost effective and robust manufacturing processes by allowing a fairly wide range of average particle size and size distribution while preserving a similarly high performance.

CRediT authorship contribution statement

Daniel Carne: Data curation, Investigation, Methodology, Writing – original draft, Writing – review & editing. Joseph Peoples: Methodology, Writing – review & editing. Fredrik Arentz: Investigation, Writing – review & editing. Xiulin Ruan: Conceptualization, Funding acquisition, Supervision, Writing – review & editing.

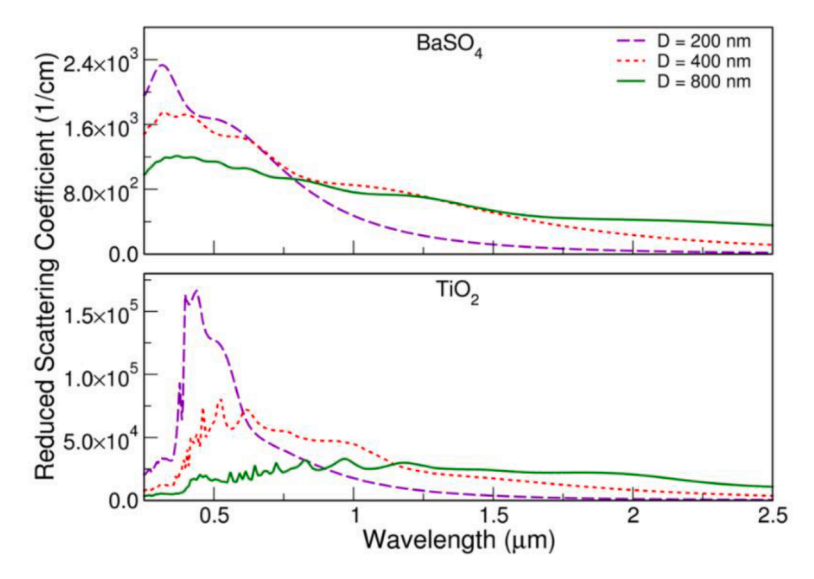


Fig. 4. Reduced scattering coefficient of BaSO₄-acrylic and TiO₂-acrylic paints at a 60 % volume fraction with nanoparticle diameters ranging from 200 to 800 nm.

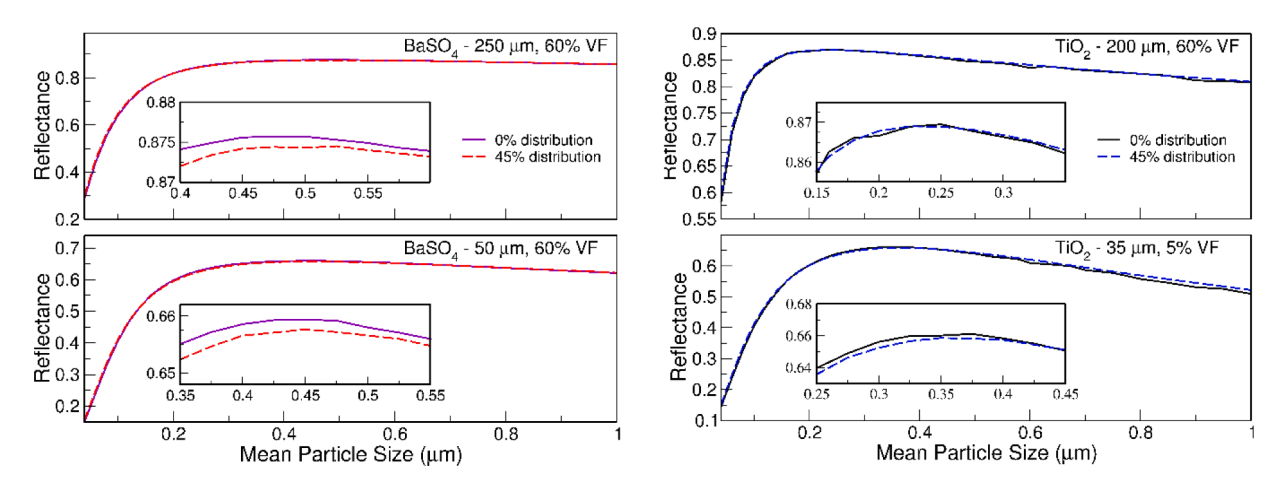


Fig. 5. Solar reflectance as a function of mean particle size for a thin (50 μ m, 60 % volume fraction) and thick (250 μ m, 60 % volume fraction) BaSO₄-acrylic paint, and a thin (35 μ m, 5 % volume fraction) and thick (200 μ m, 60 % volume fraction) TiO₂-acrylic paint.

Declaration of competing interest

The authors declare the following financial interests/personal relationships which may be considered as potential competing interests: Daniel Carne reports financial support was provided by National Science Foundation. Xiulin Ruan reports financial support was provided by National Science Foundation. Joseph Peoples reports financial support was provided by NASA. If there are other authors, they declare that they have no known competing financial interests or personal relationships that could have appeared to influence the work reported in this paper.

Data availability

Data will be made available on request.

Acknowledgments

D.C. and X.R. acknowledge partial support from the US National Science Foundation (Award #2102645). J.P. acknowledges support from the NASA Space Technology Graduate Research Opportunity Program (Grant #80NSSC20K1187).

Supplementary materials

Supplementary material associated with this article can be found, in the online version, at doi:10.1016/j.ijheatmasstransfer.2024.125209.

References

- [1] U.S. E.I.A. Annual Energy Outlook, 2022.
- [2] J. Peoples, X. Li, Y. Lv, J. Qiu, Z. Huang, X. Ruan, A strategy of hierarchical particle sizes in nanoparticle composite for enhancing solar reflection, Int. J. Heat Mass Transf. 131 (2019) 487–494.
- [3] A.W. Harrison, M.R. Walton, Radiative cooling of TiO₂ white paint, Solar Energy 20 (2) (1978) 185–188.
- [4] T.M.J. Nilsson, G.A. Niklasson, Radiative cooling during the day: simulations and experiments on pigmented polyethylene cover foils, Solar Energy Mater. Solar Cells 37 (1) (1995) 93–118.
- [5] A.R. Gentle, G.B. Smith, Radiative heat pumping from the Earth using surface phonon resonant nanoparticles, Nano Lett. 10 (2) (2010) 373–379.
- [6] Z. Huang, X. Ruan, Nanoparticle embedded double-layer coating for daytime radiative cooling, Int. J. Heat Mass Transf. 104 (2017) 890–896.
- [7] X. Li, J. Peoples, Z. Huang, Z. Zhao, J. Qiu, X. Ruan, Full daytime sub-ambient radiative cooling in commercial-like paints with high figure of merit, Cell Rep. Phys. Sci. 1 (10) (2020) 100221.
- [8] X. Li, J. Peoples, P. Yao, X. Ruan, Ultrawhite BaSO₄ paints and films for remarkable daytime subambient radiative cooling, ACS Appl. Mater. Interfaces 13 (18) (2021) 21733–21739.

- [9] M. Baneshi, S. Maruyama, H. Nakai, A. Komiya, A new approach to optimizing pigmented coatings considering both thermal and aesthetic effects, J. Quant. Spectrosc. Radiat. Transfer 110 (3) (2009) 192–204.
- [10] C.H. Wang, M.X. Liu, Z.Y. Jiang, TiO₂ particle agglomeration impacts on radiative cooling films with a thickness of 50μm, Appl. Phys. Lett. 121 (2022) 202204.
- [11] M. Chen, D. Pang, J. Mandal, X. Chen, H. Yan, Y. He, N. Yu, Y. Yang, Designing mesoporous photonic structures for high-performance passive daytime radiative cooling, Nano Lett. 21 (3) (2021) 1412–1418.
- [12] Y. Dong, H. Han, F. Wang, Y. Zhang, Z. Cheng, X. Shi, Y. Yan, A low-cost sustainable coating: improving passive daytime radiative cooling performance using the spectral band complementarity method, Renew. Energy 192 (2022) 606–616.
- [13] X. Wang, X. Liu, Z. Li, H. Zhang, Z. Yang, H. Zhou, T. Fan, Scalable flexible hybrid membranes with photonic structures for daytime radiative cooling, Adv. Funct. Mater. 30 (5) (2020) 1907562.
- [14] J.R. Frisvad, N.J. Christensen, H.W. Jensen, Computing the scattering properties of participating media using Lorenz-Mie theory, ACM Trans. Graph. 26 (3) (2007) 60.
- [15] M. Kaviany, Principles of Heat Transfer in Porous Media, Springer, New York,
- [16] K. Kamiuto, Correlated radiative transfer in packed-sphere systems, J. Quant. Spectros. Radiat. Transfer 43 (1) (1990) 39–43.
- [17] W.C. Mundy, J.A. Roux, A.M. Smith, Mie scattering by spheres in an absorbing medium, J. Opt. Soc. Am. 64 (1974) 1593–1597.

- [18] J.R. Howell, M. Perlmutter, Monte Carlo solution of thermal transfer through radiant media between gray walls, ASME J. Heat Transfer 86 (1) (1964) 116–122.
- [19] M.F. Modest, Radiative Heat Transfer, Elsevier Science, 2013.
- [20] L. Wang, S.L. Jacques, Monte Carlo modeling of light transport in multi-layered tissues in standard C, Comput. Methods Programs Biomed. 47 (2) (1995) 131–146.
- [21] ASTM G173-03, Standard Tables For Reference Solar Spectral Irradiances: Direct normal and Hemispherical on 37° Tilted Surface, 2020.
- [22] S.L. Jacques, C.A. Alter, S.A. Prahl, Angular dependence of HeNe laser light scattering by human dermis, Lasers Life Sci. 2 (4) (1988) 309–333.
- [23] L. Wang, S.L. Jacques, Use of a laser beam with an oblique angle of incidence to measure the reduced scattering coefficient of a turbid medium, Appl. Opt. 34 (13) (1995) 2362–2366.
- [24] T.C. Grenfell, A theoretical model of the optical properties of sea ice in the visible and near infrared, J. Geophys. Res. 88 (C14) (1983) 9723–9735.
- [25] T. Bäck, H. Schwefel, An overview of evolutionary algorithms for parameter optimization, Evol. Comput. 1 (1) (1993) 1–23.
- [26] R. Salomon, Evolutionary algorithms and gradient descent search: similarities and differences, IEEE Trans. Evolut. Comput. 2 (2) (1998) 45–55.
- [27] D. Carne, J. Peoples, D. Feng, X. Ruan, Accelerated prediction of photon transport in nanoparticle media using machine learning trained with Monte Carlo simulations, ASME. J. Heat Mass Transfer 145 (5) (2023) 052502.
- [28] Baneshi, M., Gonome, H., Komiya, A., Maruyama, S., 2012, "The effect of particle size distribution on aesthetic and thermal performances of polydisperse TiO2 pigmented coatings: comparison between numerical and experimental results," 113(8), pp. 594–606.